Nuclear Instruments and Methods in Physics Research A 772 (2015) 103–111

Contents lists available at ScienceDirect

Nuclear Instruments and Methods in Physics Research A

journal homepage: www.elsevier.com/locate/nima

Investigation on gamma-ray position sensitivity at 662 keV in a spectroscopic 3" x 3" $LaBr_3$:Ce scintillator

A. Giaz [a,*], F. Camera [a,b], F. Birocchi [a,b], N. Blasi [a], C. Boiano [a], S. Brambilla [a], S. Coelli [a], C. Fiorini [a,c], A. Marone [c], B. Million [a], S. Riboldi [a,b], O. Wieland [a]

[a] INFN Milano, Via Celoria 16, 20133 Milano, Italy
[b] Università degli Studi di Milano, Physics Dept., Via Celoria 16, 20133 Milano, Italy
[c] Politecnico di Milano, Dipartimento di Elettronica, Informazione e Bioingegneria, Via Golgi 40, 20133, Milano, Italy

ARTICLE INFO

Article history:
Received 14 April 2014
Received in revised form
15 September 2014
Accepted 27 October 2014
Available online 4 November 2014

Keywords:
LaBr3:Ce scintillators
Position sensitivity
Doppler broadening
Imaging

ABSTRACT

The position sensitivity of a thick, cylindrical and continuous 3" x 3" (7.62 cm x 7.62 cm) $LaBr_3$:Ce crystal was studied using a 1 mm collimated beam of 662 keV gamma rays from a 400 MBq intense ^{137}Cs source and a spectroscopic photomultiplier (PMT) (HAMAMATSU R6233-100SEL). The PMT entrance window was covered by black absorber except for a small window 1 cm x 1 cm wide.

A complete scan of the detector over a 0.5 cm step grid was performed for three positions of the 1 cm x 1 cm window. For each configuration the energy spectrum was measured and the peak centroid, the FWHM, the area and peak asymmetry of the 662 keV gamma transition were analyzed. The data show that, even in a 3" thick $LaBr_3$:Ce crystal with diffusive surfaces the position of the full energy peak centroid depends on the source position. We verified that, on average, the position of the full energy peak centroids measured in the three 1 cm x 1 cm window configurations is sufficient for the correct identification of the collimated gamma source position.

1. Introduction

The $LaBr_3$:Ce material is an inorganic scintillator which presents excellent scintillation properties. It has an extremely high light yield (63 photons/keV), the best energy resolution among scintillators (2.7% at 662 keV for small volume crystals), excellent timing properties (300 ps of time resolution) and a high density (5.1 g/cm^3) [1–20].

Due to the high light yield, these scintillators are suitable to position sensitivity applications. Scrimger and Baker showed [21,22] that, for scintillators with absorbing surfaces, the light point spread function measured at position x,y on the photocathode ($r^2=x^2+y^2$), i.e. the light distribution on the photocathode for a point-like source located at $r=0$, has a Gaussian shape whose FWHM depends on the crystal light yield and on the distance t between the scintillation point and the photocathode according to:

$$I(r)=\frac{I_0}{[1+(r/t)^2]^{3/2}} \quad (1)$$

where I_0 is the amplitude of the distribution. The interaction point depends on the probability of the gamma ray to penetrate the material. Therefore the best spatial resolution is achieved for low energy gamma rays in detectors only few millimeters thick with black absorbing surfaces. This solution is adopted to avoid signal deterioration due to the reflection/diffusion of the scintillation light. The use of absorbing surfaces, however, implies a loss in the collected scintillation light with a consequent worsening in the energy resolution, and the thinness of the crystal makes them inefficient for gamma rays of higher energies.

Several works can be found in literature which deal with the position sensitivity properties of monolithic scintillators, mostly focused on medical applications, such as Anger cameras or PET. In those cases, the devices are used to localize the emitter point with the best possible precision and a sub millimeter spatial resolution is required. On the other hand, an energy resolution of the order of 10–15% at 0.5 MeV is usually sufficient and, therefore, black surfaces are used in most of the cases.

In Anger Cameras, low energy gamma rays are employed (typically the 140 keV gamma ray from ^{99m}Tc). At these energies, the photoelectric effect predominates and detector thicknesses of the order of 5–10 mm are mostly used. We remember here the works of Pani et al. [23–29], Fabbri et al. [30–32], Alzimami et al. [33], Deprez et al. [34], Yamamoto et al. [35], Busca et al. [36] and Fiorini et al. [37].

* Corresponding author. Tel.: +39 02 50317217; fax +39 02 50317487.
E-mail address: agnese.giaz@mi.infn.it (A. Giaz).

http://dx.doi.org/10.1016/j.nima.2014.10.062
0168-9002/

In PET two coincident 511 keV gamma rays coming from positron annihilation are detected. At this energy range the Compton effect becomes important, therefore a spreading of the scintillation light might be expected. Good efficiency would require a thickness of the order of some radiation lengths, but this would imply a large error in the emitter localization because of parallax effects on one hand, and a large value of t in Eq. (1) on the other. Therefore the crystal thickness is kept below 20 mm and several techniques to determine the depth of interaction (DOI) were developed [38–43].

To our knowledge, the only experimental investigation on position sensitivity on a crystal thicker than 2 cm with diffusive surfaces was done by Busca et al. [44] who tested a gamma camera made of a 1"x1" LaBr3 crystal coupled to SDDs using a 662 keV beam from a ^{137}Cs source. They measured an energy resolution of 3% typical of such a crystal. At the same time, they found that, in spite of the 2.5 cm thickness and the diffusive surfaces, a position sensitivity is still retained on an event by event basis, being able to distinguish the source position within 5 mm.

In nuclear structure physics research, where energy resolution and efficiency for medium/high energy gamma rays are critical parameters, $LaBr_3$:Ce scintillators are giving an alternative or complementary solution to HPGe detectors due to their performances and manageability. In order to optimize the energy resolution, crystals with diffusive surfaces must be used and, since the energies of interest range from $\approx$100 keV up to $\approx$20 MeV, detectors must be much thicker than those used for SPECT or PET applications. The information on the gamma ray interaction point in the photocathode x-y plane, however, would allow a reduction of the Doppler broadening effect when the emitter moves with high or relativistic velocity [45,46]. This is the case, for example, of inverse kinematic reaction measurements with exotic beams, i.e. nuclei far from stability accelerated to velocities up to v/c=0.7 and more. In this case the energy of the emitted gamma rays is Doppler shifted in the laboratory system and, due to the size of the detector opening angle, the full absorption peak is broadened and degraded in the energy spectrum, according to the formula:

$$E'_\gamma = \frac{\sqrt{1-\beta^2}}{1-\beta cos\theta_\gamma} E_\gamma \quad (2)$$

where E_γ and E'_γ are the gamma ray energies emitted at a laboratory angle θ_γ from a source in the center of mass system moving with velocity $\beta = v/c$, respectively. For example, a 3" x 3" $LaBr_3$:Ce detector placed at 20 cm from the target covers an angle θ_γ of almost 11° and a 1 MeV gamma ray is detected with ~25 keV energy resolution if emitted by a fixed source, ~70 keV if emitted by a source moving with velocity v/c=0.3 and ~230 keV for v/c=0.7 [45].

The reduction of the Doppler broadening effect is an important issue in gamma ray nuclear spectroscopy. The most advanced HPGe arrays (such as AGATA, GRETA, MINIBALL [47–57] etc.), composed by segmented HPGe detectors, solve this problem through pulse shaping analysis and tracking technique [58–61]. This advanced technique implies a complex data analysis which allows to obtain a sensitivity of few millimeters to recover an intrinsic energy resolution of the order 0.3% at 0.5 MeV, typical of HPGe detectors. However, since the energy resolution of the $LaBr_3$:Ce scintillators is 10 times larger, a sensitivity of only about 1–2 cm, obtainable in a easier way, is estimated to be enough to correct the Doppler broadening maintaining the intrinsic energy resolution of the scintillator.

It is the aim of this work to investigate whether large 3" x 3" LaBr3 crystals with diffusive surfaces retain position sensitivity for medium/high gamma rays. As observed in Ref. [44], diffusive surfaces in thick crystals produce a background due to reflected scintillation light which is expected to increase with the dimension of the crystal. Furthermore, medium/high energy gamma rays entering in the crystal interact several times through Compton interaction and each gamma ray will deposit energy in more than one position inside the crystal. The scintillation light produced in these interaction points has to travel several centimeters inside the crystal before reaching the photocathode. Ref. [13,19] report that the average mean path of scintillation light is 45 cm for a 3" x 3" crystal with diffusive surfaces. In a 3" x 3" $LaBr_3$:Ce the scintillation light which illuminates directly the photocathode is approximately seven times less intense than the light diffused by the crystal surfaces [62].

In order to investigate whether position sensitivity is still retained in a 3" x 3" diffusive surfaces crystal and how it depends on the gamma energy, we performed simple Monte Carlo simulations, presented in Section 2, on the spatial distribution of the energy released by gamma rays of energies from 100 keV to 5 MeV. We found that, on average, the spreading of the energy deposited by the gamma ray is limited to a narrow region around the scintillation point with a width still sufficient to recover the spatial information for energies larger than 400 keV and that the distribution of scintillation light on the detection plane is still sensitive to the position of the scintillation point for medium/high gamma energies.

We then performed a set of measurements, described in Section 3, using a 3" x 3" $LaBr_3$:Ce coupled to a photomultiplier (PMT) shielded by a black absorber, in which only an area of 1 cm x 1 cm was left uncovered, and a collimated monochromatic 662 keV gamma ray source (400 MBq ^{137}Cs).

It is important to remember that in nuclear physics experiments the position of the emitter is well known and position sensitivity is used as an additional observable (together with energy and time) to determine the angle of emission of the measured gamma ray. As detectors are usually placed at ~20 cm or more from the target (the gamma source) the parallax error due to the crystal dimensions is at most 5 mm, well below the precision of 1–2 cm required to recover the intrinsic energy resolution of the detectors. Therefore, in this work we will neglect the parallax effect and consider only gamma rays which enter perpendicularly on the detector front face.

The results of the measurements, discussed in Section 4, showed characteristic patterns and were then used to reconstruct the position of the source in new measurements, presented and discussed in Section 5. We want to emphasize that neither the experimental setup nor the experimental techniques used in this work are meant to be used in a real nuclear physics experiment. Our aim is to investigate whether large volume 3" x 3" $LaBr_3$:Ce spectroscopic detectors with diffusive surfaces maintain a position sensitivity to medium/high gamma rays of the order of 1–2 cm. Once the sensitivity is proved, a detection system with position sensitive light sensors and an appropriate algorithm to recover the position of the scintillation point on an event by event basis should be developed. Conclusions are drawn in section 6.

2. Monte Carlo simulations

As a first step to study the position sensitivity of a 3" x 3" $LaBr_3$:Ce scintillator a series of simulations were performed to check if the energy deposition of the incident gamma ray maintains the information on its original direction (the multiple hits inside the crystal and the consequent multiple light sources spots might degrade/cancel the positional information) and ii) if the scintillator light transport from the multiple light sources spots up to the photocathode still maintains the information on the original direction of the incident

gamma ray (in fact the diffusion on the surfaces of ~85% of the collected scintillation photons degrades the positional information).

A preliminary study was performed on a 1" x 1" and a 3" x 3" cylindrical crystal [63,64]. Following that work, a simulation of the gamma ray interactions in the scintillation material was performed in order to study the spreading of the energy deposited by a gamma ray in a 3" x 3" cylindrical $LaBr_3$:Ce scintillator. Considering a coordinate system with the origin in the center of the front face, the x-y plane coincident with the front face opposite to the PMT and the z-axis along the cylindrical symmetry axis (see Fig. 1), we first analyzed how the energy release is spatially distributed for a dimensionless monochromatic beam of gamma rays incident perpendicularly to the x-y plane.

Several energies of the gamma rays were simulated, i.e. 121 and 344 keV, corresponding to transitions of the ^{152}Eu source, 662 keV, corresponding to the ^{137}Cs transition, 1332 keV, corresponding to a ^{60}Co transition, 2.5, 5 and 20 MeV. Fig. 2 shows the distribution of the deposited energy projected on the x-axis when the gamma beam enters perpendicularly at the origin of the coordinate system (for symmetry reasons the projection on the y-axis is similar). It turns out that the distributions have a Gaussian-like shape centered around the source position. Similar results were obtained when the beam was located at 1, 2 or 3 cm from the center (not shown), where the Gaussian is centered around 1, 2 or 3 cm from the center, respectively. It is interesting to observe that most of the energy released is concentrated within one centimeter independently on the type of gamma interaction mechanism involved the various energies (photoelectric, Compton or Pair production). The Fig. 3 shows the percentage of energy released in the x range (−0.5 cm, 0.5 cm) (open squares) or (−1 cm, 1 cm) (full circles) as a function of incident gamma energy. For low energies, where the photoelectric effect dominates, 99% of the energy is released within a 1 cm wide interval. As the Compton effect becomes important the energy is released over a larger area. Nevertheless at 662 keV more than 80% is released within a 1 cm wide interval, and more than 90% within a 2 cm wide one. When the energy increases, the Compton scattering becomes more forward directed until pair production becomes possible widening the area where the energy is released. In all cases 80% to 90% of the energy is released within 1 cm.

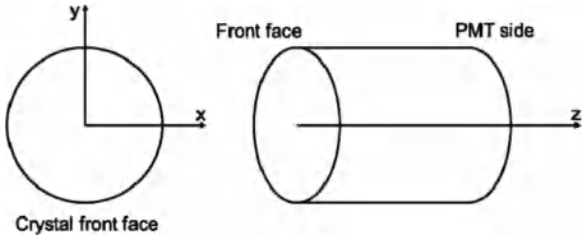

Fig. 1. The coordinate system used for the simulation and for the measurements.

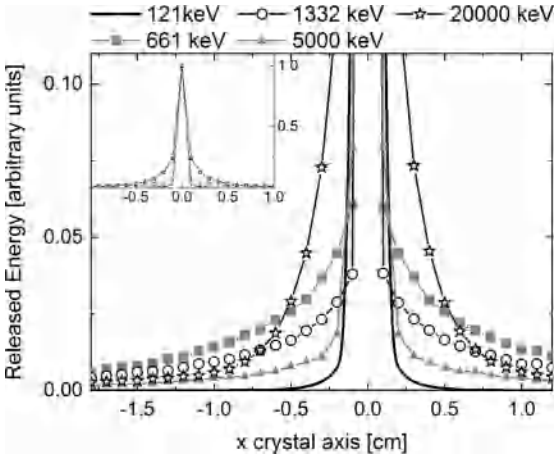

Fig. 2. The simulated released energy distribution projected on the x-axis is shown for several γ-ray energies. For all energies the maximum is set to one. The γ-ray beam is positioned in the origin. The scale of the y-axis is cut to 12% in order to better distinguish the different curve behaviors. The inset shows the full picture. The black line refers to 121 keV γ rays, the gray full squares to 662 keV, the open circles to 1332 keV, the gray triangles to 5 MeV and the open stars to 20 MeV γ rays.

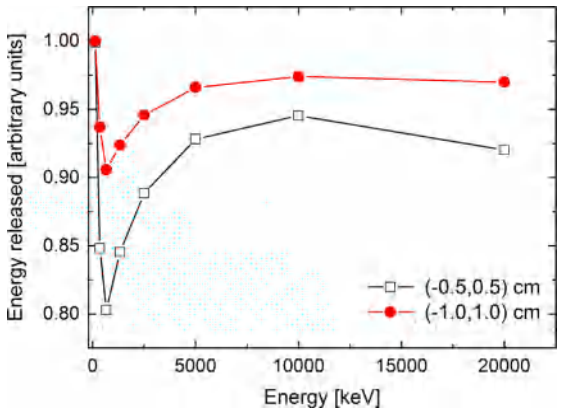

Fig. 3. The percentage of energy released within the x range (−1 cm, 1 cm) (full circles) or (−0.5 cm, 0.5 cm) (open squares) is shown as a function of incident γ energy. The γ ray beam is positioned in the center of the front face as in Fig. 2.

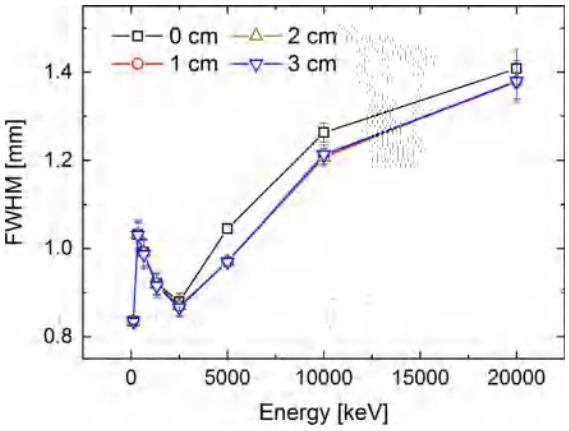

Fig. 4. The FWHM of the released energy distribution of Fig. 2 is shown as a function of the γ ray energy. Open squares refer to the case of the source located in the center of the detector front face. The cases of the source positioned at 1, 2 or 3 cm from the center are perfectly overlapping, and are represented by open triangles.

Similarly, the FWHM of the distribution of Fig. 2, as a function of the gamma-ray energy, is shown in Fig. 4 for several beam positions. It diminishes between 0.5 and 2.5 MeV because of the forward directed Compton effect. When pair production starts to be important, the energy release distribution widens again, with a slightly larger effect in the case of a centered beam.

The distribution of deposited energy along the z-axis depends mainly on the gamma-ray energy, as it is shown in Fig. 5. For energies around 100 keV the distribution is peaked at few millimeters from the detector surface. As the energy increases, the maximum of the distribution moves deeper into the scintillator, but it is less and less pronounced. Combining the x-y and z distributions, we find that for energies around 100 keV the interaction point is well localized both in the x-y plane and in depth, but, according to the Scrimger and Baker relation (Eq. (1)) [21,22], the distance between this point and the photomultiplier is too large to retain the position information at the photomultiplier cathode.

As the energy increases, the probability of energy release is more and more spread over the z-axis.

These results here define the limit for on the best possible position sensitivity which could be obtained on average in an ideal case. In fact, we cannot expect a position sensitivity better than the light spot size produced by the gamma beam.

As a second step of the simulation work, in order to have an indication on how the diffusive surfaces affect the scintillation light distribution on the detection plane, we performed simple simulations using the code SCIDRA [65], in which the scintillation photons produced in the interaction process are transported to the photocathode. In the simulation, surfaces were assumed diffusive and the reflecting indexes of the crystal, the sealing glass, the optical grease and the phototube glass were taken into account. The resulting scintillation light distributions on the detection plane are shown in Fig. 6 for the gamma source positioned in the center (x, y)=(0 cm, 0 cm) or in (x, y)= (2 cm, 0 cm), respectively. The spectra of Fig. 6 were normalized at $x=-40$ mm in order emphasizes the correlation between the gamma rays interaction position and the scintillation light distribution at the cathode. It turns out that in both cases there is no position sensitivity for gamma energies below ≈ 400 keV, due to the distance of the scintillation point from the detection surface. For larger energies the position sensitivity is clearly observed. This results indicate that it might be possible to extract the information on the scintillation position also in a 3" x 3" $LaBr_3$:Ce crystal with diffusive surfaces for medium/high gamma energies.

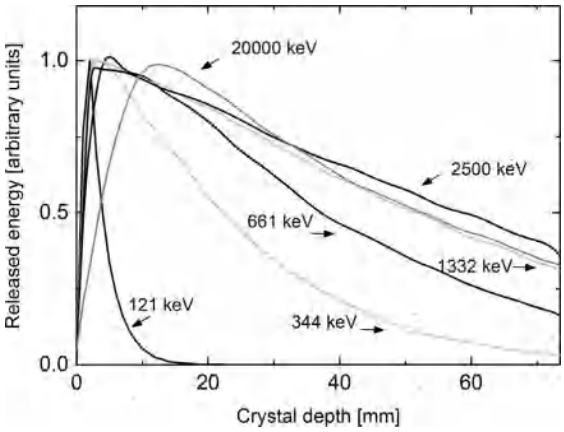

Fig. 5. The energy released in the crystal as a function of the detector deepness is shown for several gamma-ray energies. The zero corresponds to the front face. The source is in front of the detector center. The maximum of each curve is normalized to 1. The curve fluctuations have a statistical nature.

3. The measurements

In order to verify experimentally the simulation results, we performed a set of measurements using a 3" x 3" $LaBr_3$:Ce crystal (S/N J79CsB). The crystal we used for the measurements is a commercial one delivered by Saint Gobain sealed in a frame with diffusive surfaces in order to collect all the scintillation light and obtain the best energy resolution. We assume that the crystal material is homogeneous. LaBr3:Ce has internal radiation due to ^{138}La and ^{227}Ac [14]. Such radiation produces a background which, in the spectra presented in this work is ~8% of the total events. In the measurements the dead time was less than 2%. In nuclear physics experiments, such a background is totally eliminated when coincidence with beam or with other ancillary detectors is requested or it can be easily subtracted by measuring a spectrum without the source.

The rear transparent face was coupled to the spectroscopic photomultiplier (PMT) HAMAMATSU R6233-100SEL (S/N DA1382). This PMT has a cathode luminous sensitivity of 148 μA/lm and a cathode blue sensitivity index of 16.1. The PMT was coupled to an HAMAMATSU E1198-26 voltage divider (VD). The detector is commonly used in nuclear spectroscopic measurements, with a typical energy resolution of 20 keV (FWHM) at 662 keV (see Fig. 7), namely 3%, which corresponds to the value quoted in the Saint Gobain detector datasheet.

In order to study how the scintillation light distribute on the detection plane as a function of the gamma source position, the photocathode entrance window was shielded by means of a black tape with a square window of 1 cm x 1 cm area, as can be seen in Fig. 8. We verified the absorption properties of the tape by performing a test measurement with no window in the shield. Three positions of the window were considered: i) in the center of the PMT (position A), ii) at 1.5 cm from the center (position B) and iii) at 3 cm from the center of the PMT along the x-axis (position C), as shown in Fig. 8.

The collimated gamma ray source, ^{137}Cs, with an intensity of 400 MBq, was completely shielded and collimated by lead and heavy met [66]. The collimator was 8 cm long with a hole diameter of 1 mm, so that 96% of the γ rays hitting the detector were collimated within a 1 mm wide beam spot. The source was fixed on a platform which could be moved both along the x- and the y-axes through a micrometer screw. Care was taken that the gamma ray beam was perpendicular to the detector front face.

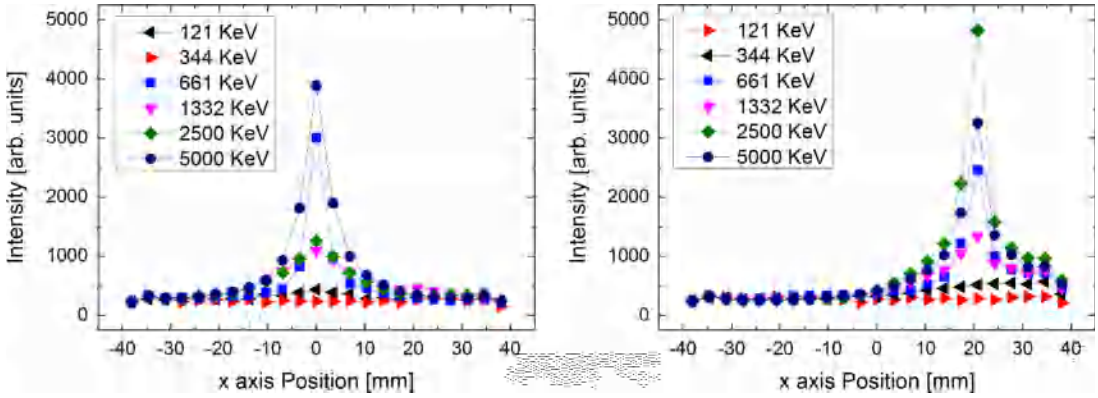

Fig. 6. Intensity distribution of the scintillation light as measured on the photocathode for gamma rays of energy from 121 keV up to 5 MeV. In the left panel the source is in position (x, y)=(0 cm, 0 cm), in the right panel the source is in position (x, y)=(2 cm, 0 cm) and in both plots the curves have been normalized to have the same intensity at $x=-40$ mm.

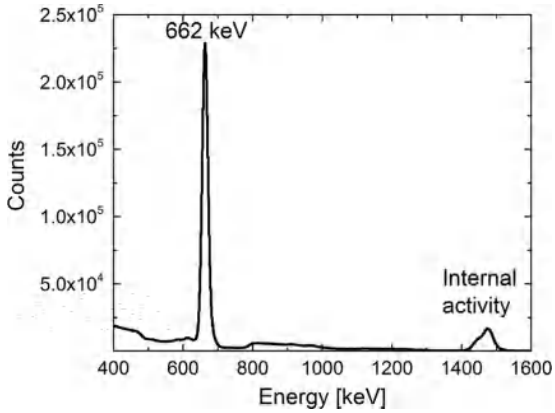

Fig. 7. The energy spectrum of ^{137}Cs measured without the shield on the PMT is shown. The energy resolution (FWHM) is 20 keV at 622 keV (3%). The internal radioactivity coming from the decay of ^{138}La, present in the crystal, is visible.

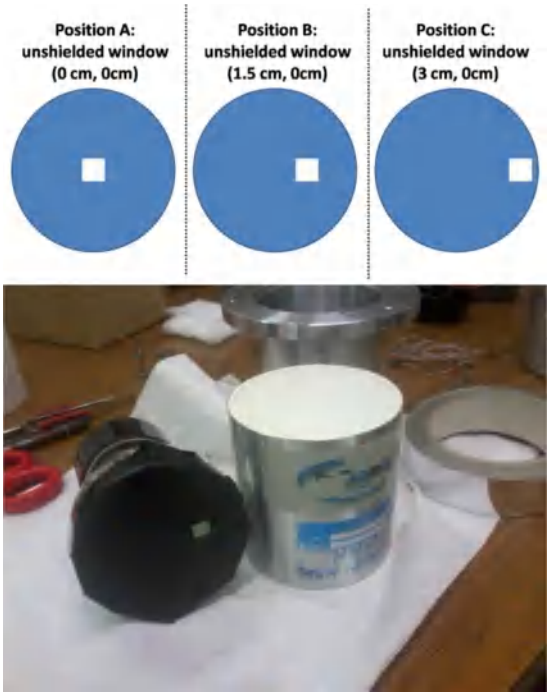

Fig. 8. In the top panel the positions (labeled A, B and C) of the three windows on the photocathode entrance window are represented. The photo shows the $LaBr_3$:Ce crystal and the shielded PMT. The window is at 1.5 cm from the center along the x-axis (position B).

The distance between the detector surface and the collimator was about 1.5 cm.

A high voltage of −600 V was applied on the detector through a CAEN N1470 4 channel HV power supply. Data were taken using a TENNELEC TC 244 spectroscopy amplifier and an ORTEC 926 MCA.

A set of measurements were performed moving the collimated 662 keV gamma ray source along a 0.5 cm grid. About 180 energy spectra were acquired.

The peak of the 662 keV transition was fitted by a Bigaussian curve, due to its asymmetric shape (see Fig. 9). The Bigaussian curve is the combination of two different Gaussians with different sigma, one applied to the values smaller than the centroid (left Gaussian) and the other to the values larger than the centroid (right Gaussian). A Bigaussian fit gives the following parameters: the position of the centroid, the peak height, the two half sigma (called sigma left and sigma right), and the area. We studied the sensitivity to the source position of the various parameters of the full energy peak: the centroid (related to the average number of measured photo-electrons), the FWHM, the asymmetry, i.e. the ratio between sigma left and sigma right, and the area of the full energy peak.

The position of the centroid turns out to be sensitive to the position of the source, as can be seen in Fig. 9 and discussed in the next section. The gamma source is placed at $x=0$ and moved along the y-axis in 0.5 cm steps from −3.5 cm (bottom curve) to 0 cm (top curve). In order to make the picture clear, we added a different offset in the y-scale to each curve. One can see that when the γ beam is exactly in front of the window, the centroid is located at the highest channel value (green curve in the on line version), and it moves to lower values as the source moves away from the window.

We additionally analyzed the other properties of the full energy peak to search for a γ ray position dependence.

In Fig. 10 we show a 3D plot of the energy resolution as a function of the source position for the window in position A. It can be seen that the energy resolution does not change significantly. It should be noted that, due to the shielding, the energy resolution of the detector worsens drastically. However, here our aim is to investigate how the scintillation light distributes on the detection surface as a function of the source position. Fig. 11 shows the area

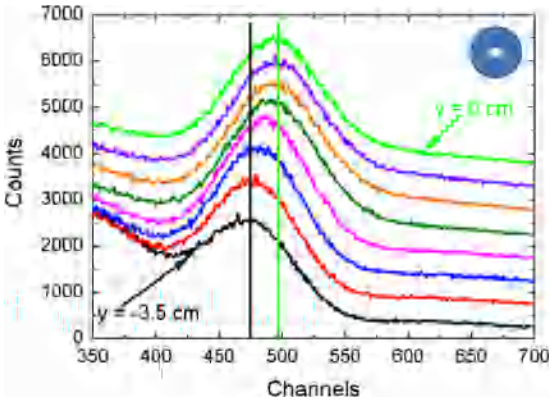

Fig. 9. The measured energy spectra with the window in the center of the photocathode (position A) are shown. A y-offset was added to the curves corresponding to different source positions, for a better view. The source was placed at 0 cm from the center along the x-axis, and moved along the y-axis, from −3.5 cm (bottom curve) to 0 cm (top curve) in 0.5 cm steps. The spectra were acquired with the same live time of 600 s. The dependence of the centroid position on the position of the source is evident.

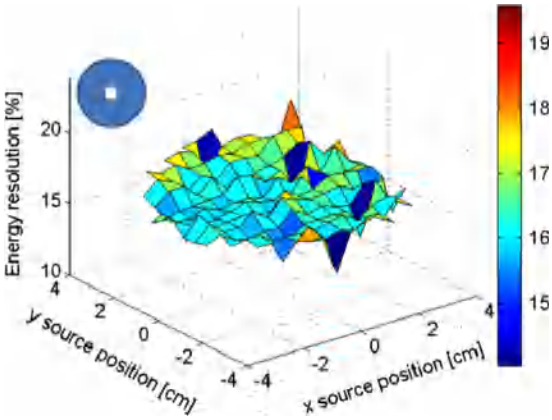

Fig. 10. The energy resolution is shown as a function of the source position. The window was placed at the center of the photocathode, as indicated in the inset. For a clearer view colors were introduced, the color legend is on the right side and refers to the energy resolution (z-axis).

of the full energy peak as a function of the source position, again for the window in position A. It is interesting to note that the larger values are surrounding the real source position. This could be explained by the fact that at this energy, 662 keV, the released energy shifted laterally by the Compton scattering is not negligible, as can be inferred from Fig. 4. However, the difference between the maximum and the local central minimum in Fig. 11 is only $\approx 10\%$, and the overall picture does not show a gamma source position dependence strong enough. Also the asymmetry, i.e. the ratio between sigma left and sigma right, shows only a weak position sensitivity, as can be seen in Fig. 12.

The most effective full energy peak property to identify the position of the γ ray interaction point turns out to be the peak centroid, as we already observed in Fig. 9. The Fig. 13 shows the 3D plots of the centroid for the three window positions A (top panel), B (center panel) and C (bottom panel). The position sensitivity is quite evident for the window positions A and C. In particular, the window position A gives a radial information about the source position, while position C seems to locate the x-coordinate with rather high precision. For the window position B, although the sensitivity is also clearly observed, oscillations are observed along the x directions. Large uncertainties are therefore expected in this case.

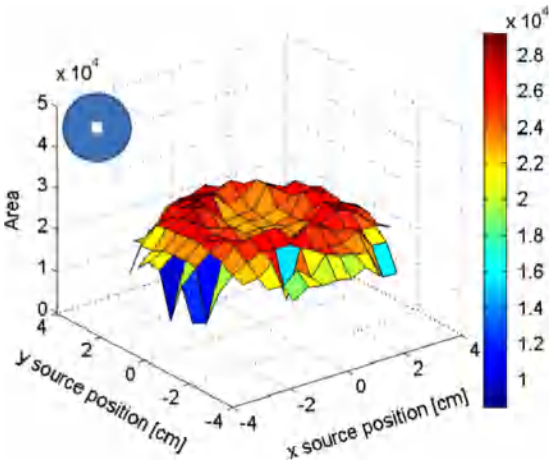

Fig. 11. The area of the full energy peak is shown as a function of the source position. The window was placed at the center of the photocathode, as indicated in the inset. For a clearer view colors were introduced, the color legend is on the right side and refers to the area (z-axis).

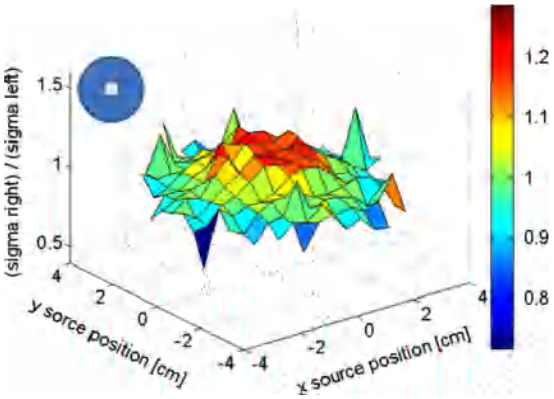

Fig. 12. The ratio of sigma left and sigma right is shown as a function of the source position. The window was placed at the center of the photocathode, as indicated in the inset. For a clearer view colors were introduced, the color legend is on the right side and refers to the sigma left and sigma right ratio (z-axis).

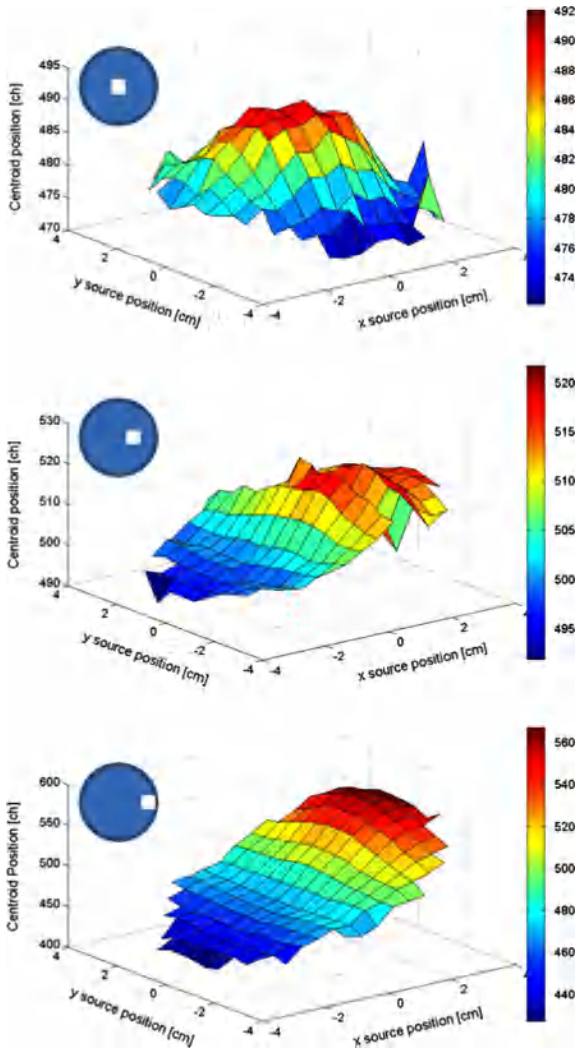

Fig. 13. The positions of the full energy peak centroid as a function of the source position is shown. In the top panel the shield window was in position A, as shown in the inset; in the central panel the window was in position B and in the bottom panel the window was in position C. For a clearer view colors were introduced, the color legend is on the right side and refers to the centroid position (z-axis).

The information of Fig. 13 can be used by tabulating the data into tables we will call 'look up tables'. We will then compare the results of "blind" measurements, in which the γ source position is not known "a priori", with the look up tables, as described in the next section.

Since all the three windows here considered lie on the $y=0$ axis, no accurate information could be inferred from them on the y coordinate of the γ source. However, due to the crystal cylindrical geometry, the information in the y coordinate can be obtained by rotating by 90° the coordinates of the look up tables. This has been done for the window position C, obtaining a deduced look up table corresponding to the window position $x=0$ cm, $y=3$ cm, that we label as position D.

4. Experimental tracking of the source position

In order to check whether the position dependence observed in Fig. 13 is sufficient to extrapolate the gamma source position, we performed a set of measurements in which the energy of the incident radiation was known but the position of the gamma source was not known "a priori" (called "blind" measurement).

Each "blind" measurement actually consisted of four measurements with windows in the four positions corresponding to the look up tables (A, B, C and D). In order to have a good normalization and to check for possible drifts, each measurement was preceded and followed by a calibration run with the source in different known positions. We repeated this procedure for three unknown positions of the gamma source.

The procedure to identify the position of the incident γ ray will be explained for one "blind" measurement while the results of all "blind" measurements are reported at the end of the section.

The measured centroids of the 662 keV peak of the first "blind" measurement were compared to the centroids in the look up tables. This comparison is shown in Figs. 14 and 15, were the projections of the 3D plots of Fig. 13 are shown for the windows positions A, B, C and D. In the figure, not all points are drawn for clearness. The centroid positions measured in the "blind" measurements corresponding to each window are represented by a black line (the error bars by dashed black lines) in each plot. For each window position, the results of the "blind" measurement overlaps, within the error bars, with a number of tabulated points. We selected the coordinates of these overlapping points, and plotted them on a 2-dimensional graph representing the detector front face. The results are shown in Fig. 16 with different colors and shapes for the four window positions (A (blue squares), B (gray squares), C (red triangles) and D (pink circles)). It can be seen that each window position identifies a region of possible scintillation positions, in particular position A identifies a ring region, position B identifies half detector portion, and positions C and D identify a stripe along their direction from the center. The position of the scintillation point is expected to lie in the intersection area of all the identified regions. Figuratively, the estimated position of the gamma source is given by the overlap of the four coordinates identified by the different window positions measurements. Since the coordinates step was 0.5 cm, the

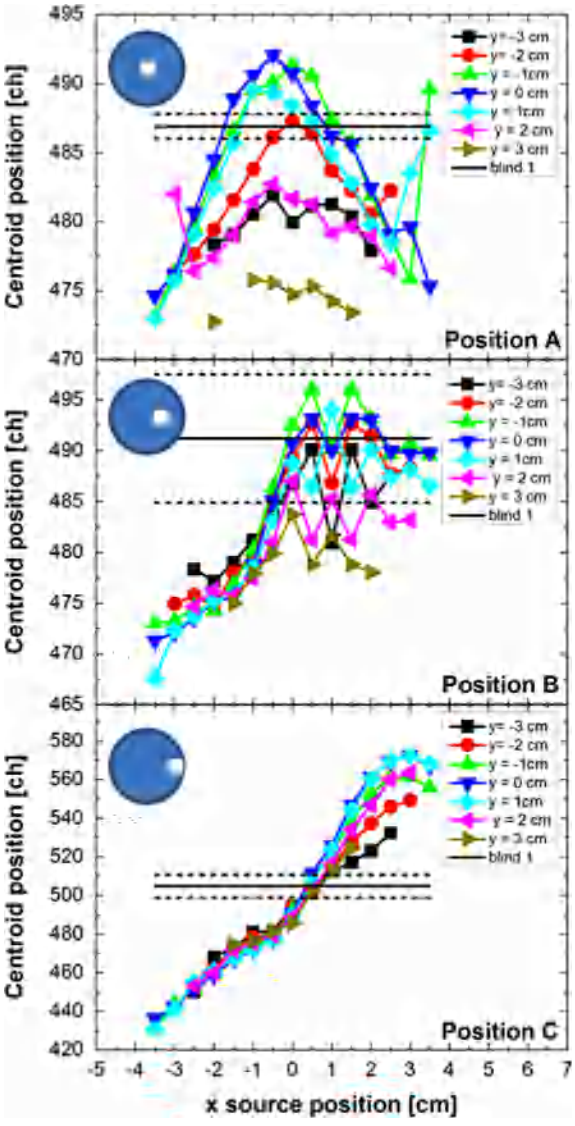

Fig. 14. The positions of the full energy peak centroid obtained in the "blind" measurements (black lines) are compared with the tabulated centroids as a function of the source position along the x-axis. The error bars of the "blind" measurements are represented by the dashed black lines. In the top panel the results relative to the window in position A; in the central and in the bottom panel the window was in position B and C, respectively.

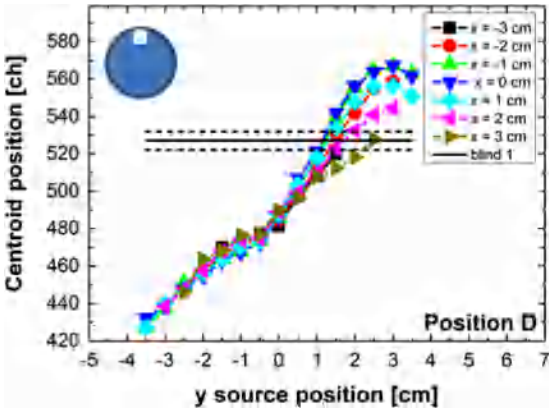

Fig. 15. The position of the full energy peak centroid obtained in the "blind" measurement (black line) with the window in position D (shown in the inset) is compared with the tabulated centroids. The error bar of the "blind" measurement is represented by the dashed black lines.

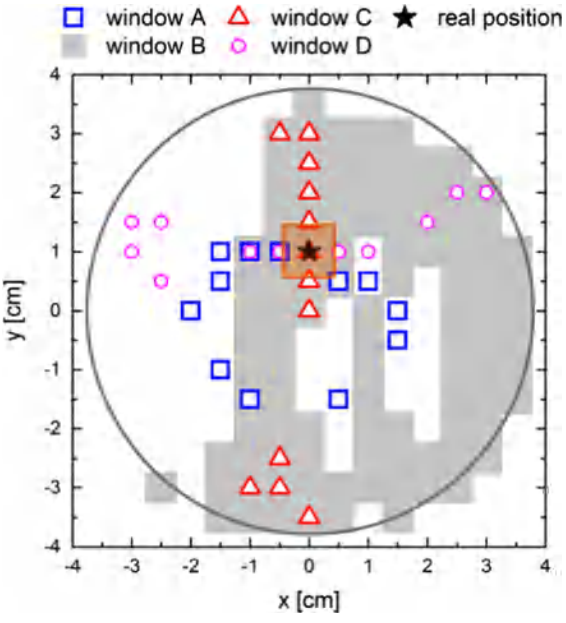

Fig. 16. The figure shows the summary of the gamma source position identification for the first "blind" measurement. The circle represents the detector front surface. The blue squares are the coordinates of the possible gamma source position points obtained with the window position A, gray area, the red triangles and the pink circles are the coordinates obtained for positions B, C and D, respectively. The orange area is the estimated region were the source is located, given by the overlap of all the sets of coordinates, assuming an uncertainty of 0.5 cm.The real position of the γ source is represented by a black star.

precision is roughly estimated to be ($x \pm 0.5$ cm, $y \pm 0.5$ cm), which corresponds to the orange area in the figure. Note that it has the same size of the open window on the PMT, and no algorithm has been applied to make it smaller. It can be seen that, while the data relative to the window position B cover a large surface, and are therefore of little use, the data relative to window A, C and D identify with great precision the actual position of the gamma source, indicated by a black star in the figure.

The same procedure was applied to two other "blind" measurements. The results are reported in Fig. 17 and in Fig. 18, where we omitted the data relative to the window position B. One can see that in all cases the estimated position of the gamma source is in excellent agreement with the real one.

Summarizing, we have shown that the full energy peak centroid is a position sensitive quantity. Look up tables with the window in few different positions can be used to retrace the gamma-ray source position:

1. The light collected in the center of the crystal (windows A) gives a radial information on the position of the γ source.
2. The light collected at the edge of the crystal on the x or y directions gives a precise information on the x or y coordinate, respectively.
3. By combining the information of only three windows positions (A, C and D) one is able to estimate with good precision the position of the gamma source.

The light collected at an intermediate radius (position B) from the crystal center do not seem to bring relevant information. The reason of this has to be further investigated.

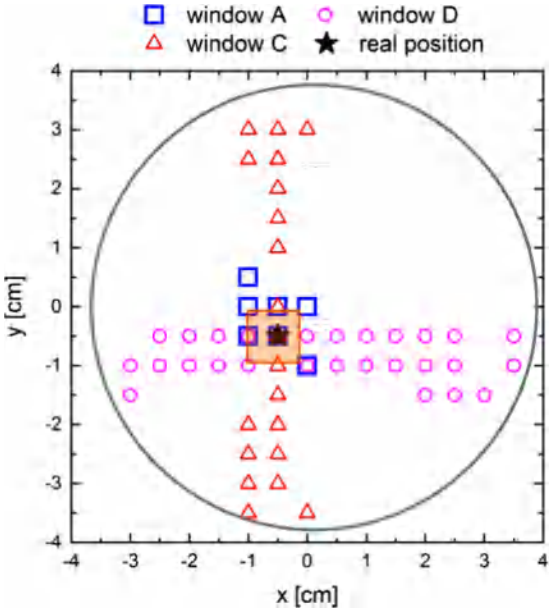

Fig. 17. Same as Fig. 16 for a second "blind" measurement. The data relative to the window position B were omitted because not relevant (see text).

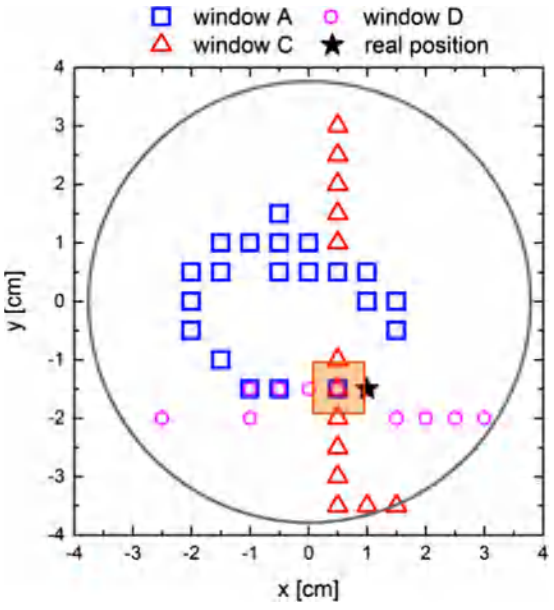

Fig. 18. Same as Fig. 16 for a third "blind" measurement. The data relative to the window position B were omitted because not relevant (see text).

5. Conclusions and perspectives

In this work we investigated whether position sensitivity is maintained in case of large volume 3" x 3" $LaBr_3$:Ce crystals with diffusive surfaces. Nowadays these crystals are more and more often used in nuclear physics spectroscopy due to their good energy resolution and efficiency. The possibility of extracting the gamma position information, besides the gamma energy and timing, would be important for a Doppler broadening correction in measurements with moving sources. We first performed Monte Carlo simulations showing that for medium/high gamma energies these crystals should still retain a position sensitivity, in spite of their dimensions and diffusive surfaces. We then verified experimentally these results using a 3" x 3" $LaBr_3$:Ce detector with diffusive surfaces coupled to a spectroscopic PMT (HAMAMATSU R6233-100SEL) and a collimated ^{137}Cs source (662 keV gamma rays). In order to study how the scintillation light distribution on the detection surface depends on the source position, we shielded the entrance window PMT by black tape with a 1 cm x 1 cm window and moved both the position of the window and the position of the collimated source. It was shown that among the several properties of the full energy peak (centroid, area, FWHM, etc.) the centroid position is the most source position sensitive one. Look up tables were built performing sets of measurements at different source positions (0.5 cm grid). Each look up table corresponds to a window position (A, B and C). By means of the comparison with these look up tables, the gamma source position in "blind" measurements could be identified with good precision. We therefore demonstrated that large volume crystals with diffusive surfaces retain a position sensitivity sufficient to identify the position of a medium energy gamma ray within 1 cm. It should be noted that the method presented here is not meant to be used in common nuclear physics experiments, since data were treated on average and not event by event, but it represents a starting point. The use of a position sensitive PMT (PSPMT), which could be a development of this work, is expected to provide the same or probably a better position sensitivity. The reconstruction of the gamma source position on an event by event basis has to be investigated, as only in this way it will be possible to use it to reduce the Doppler Broadening effect in nuclear physics experiments.

Acknowledgments

The project is co-financed by the European Union and the European Social Fund. This work was also supported by *NuPNET - ERA-NET* within the NuPNET GANAS project, under grant agreement No. 202914 and from the European Union, within the "7th Framework Program" FP7/2007-2013, under grant agreement No. 262010 – ENSAR-INDESYS. This work was also supported by

"Programmi di Ricerca Scientifica di Rilevante Interesse Nazionale" (PRIN) number 2001024324_01302

References

[1] BrilLanCe scintillators performance summary.pdf. ⟨http://www.detectors.saint-gobain.com/Brillance380.aspx⟩.
[2] E.V.D. van Loef, et al., Appl. Phys. Lett. 79 (2001) 1573.
[3] E.V.D. van Loef, et al., Nucl. Instr. Meth A486 (2002) 254.
[4] W. Moses, Nucl. Instr. Meth A487 (2002) 123.
[5] P. Dorenbos, et al., IEEE TNS. 51 (2004) 1289.
[6] B.D. Milbrath, et al., IEEE TNS 53 (2006) 3031.
[7] A. Iltis, et al., Nucl. Instr. Meth A563 (2006) 359.
[8] M. Moszynski, et al., Nucl. Instr. Meth A567 (2006) 31.
[9] M. Moszynski, et al., Nucl. Instr. Meth A568 (2006) 739.
[10] S. Normand, et al., Nucl. Instr. Meth A572 (2007) 754.
[11] A. Owens, et al., Nucl. Instr. Meth A572 (2007) 785.
[12] F. Quarati, et al., Nucl. Instr. Meth A574 (2007) 115.
[13] P. Menge, et al., Nucl. Instr. Meth A579 (2007) 6.
[14] R. Nicolini, et al., Nucl. Instr. Meth A582 (2007) 554.
[15] F.C.L. Crespi, et al., Nucl. Instr. Meth A620 (2009) 520.
[16] M. Ciemala, et al., Nucl. Instr. Meth A608 (2009) 76.
[17] M. Nocente, et al., Rev. Sci. Instrum 81 (2010) 10D321.
[18] M. Nocente, et al., IEEE Trans. Nucl. Sci. 60 (2013) 1408.
[19] A. Giaz, et al., Nucl. Instr. Meth A729 (2013) 910.
[20] I. Mazumdar, et al., Nucl. Instr. Meth A705 (2013) 85.
[21] J.W. Scrimger,, R.G. Baker, Phys. Med. Biol. 12 (1967) 101.
[22] R.G. Baker,, J.W. Scrimger, Phys. Med. Biol. 12 (1967) 51.
[23] R. Pani, et al., Nucl. Instr. Meth. A. 576 (2007) 15.
[24] R. Pani, et al., Nucl. Instr. Meth A571 (2007) 187.
[25] R. Pani, et al. (MIC conference records), IEEE NSS (2008) 1763.
[26] R. Pani, et al., Nucl. Instr. Meth. Phys. Res. 567 (2006) 294.
[27] R. Pani, et al., Nucl. Instr. Meth A576 (2007) 15.
[28] S. Lo Meo, et al. (Proc. Suppl.), Nucl. Phys. B 97 (2009) 378.
[29] R. Pani, et al., Nucl. Phys B215 (2011) 324.
[30] A. Fabbri, et al. (MIC conference records), Ieee Nss (2010))1329.
[31] A. Fabbri, et al., J. Instr 8 (2013) C02022.
[32] A. Fabbri, et al., J. Instr 8 (2013) P12010.
[33] K.S. Alzimami, et al., Nucl. Instr. Meth A633 (2011) S282.
[34] K. Deprez, et al., IEEE Trans. Nucl.Sci. 60 (2013) 53.
[35] S. Yamamoto, et al., Nucl. Instr. Meth A622 (2010) 261.
[36] P. Busca, et al. (MIC conference record), IEEE NSS (2012) 1937.
[37] C. Fiorini, IEEE Trans. Nucl. Sci. 59 (2012) 537.
[38] Van Dam, et al., IEEE Trans. Nucl. Sci. 58 (2011) 2139.
[39] Z. Li, et al., Phys. Med. Biol. 55 (2010) 6515.
[40] G. Llosa, et al., IEEE Trans. Nucl. Sci. 56 (2009) 2586.
[41] G. Llosa, et al., Nucl. Instr. Meth A702 (2013) 3.
[42] M. Carles, et al., Nucl. Instr. Meth A695 (2012) 317.
[43] M. Morrocchi, et al., Nucl. Instr. Meth A732 (2013) 603.
[44] P. Busca, et al., J. Instr 9 (2014) C05005.
[45] H.J. Wollersheim, et al., Nucl. Instr. Meth. A. 637 (2005) 637.
[46] O. Wieland, et al., Phys. Rev. Let 102 (2009) 092502.
[47] A. Gadea, et al., Nucl. Instr. Meth. A654 (2011) 88.
[48] S. Akkoyun, et al., Nucl. Instr. Meth. A668 (2012) 26.
[49] F.C.L. Crespi, et al., Nucl. Instr. Meth. A705 (2013) 47.
[50] V. Vandone, et al., Phys. Rev. C88 (2013) 044335.
[51] E. Farnea, et al., Nucl. Instr. Meth. A621 (2010) 331.
[52] F.C.L. Crespi, et al., Nucl. Instr. Meth. A604 (2009) 604.
[53] F.C.L. Crespi, et al., Nucl. Instr. Meth A570 (2007) 459.
[54] I.Y. Lee, et al., Rep. Prog. Phys. 66 (2003) 1095.
[55] I.Y. Lee, et al., Nucl. Phys. A. 746 (2004) 255C.
[56] J. Eberth, et al., Prog. Part. Nucl. Phys. 46 (2001) 389.
[57] D. Habs, et al., Prog. Part. Nucl. Phys. 38 (1997) 111.
[58] J. van der Marel,, B. Cederwall, Nucl. Instr. Meth. A437 (1999) 538.
[59] O. Wieland, et al. (Mic conference records), EEE NSS (2001) 296.
[60] O. Wieland, et al., Nucl. Instr. Meth. A487 (2002) 441.
[61] A. Lopez-Martens, et al., Nucl. Instr. Meth. A533 (2004) 454.
[62] F. Birocchi, et al. (MIC conference records), IEEE NSS (2010))198.
[63] F. Birocchi, et al. (MIC conference records), IEEE NSS (2009) 1403.
[64] F. Birocchi, Proprietà di imaging gamma con scintillatori di LaBr3 (BachelorThesis), University of Milan (2008).
[65] L. Boschini,, C. Fiorini, IEEE. Nucl. Sci. Symposium 1 (1999) 464.
[66] ⟨http://www.wolfmet.com/documents⟩.